# Major-Groove-Halogenated DNA: The Effects of Bromo and Iodo Substituents Replacing H–C(7) of 8-Aza-7-deazapurine-2,6-diamine or H–C(5) of Uracil Residues

by **Georg Becher**, **Junlin He**, and **Frank Seela***

Laboratorium für Organische und Bioorganische Chemie, Institut für Chemie, Universität Osnabrück, Barbarastrasse 7, D-49069 Osnabrück (fax: +49-(0)541-969-2370; e-mail: Frank.Seela@uni-osnabrueck.de)

Oligonucleotides containing halogenated 'purine' and pyrimidine bases were synthesized. Bromo and iodo substituents were introduced at the 7-position of 8-aza-7-deazapurine-2,6-diamine (see **2b**,**c**) or at the 5-position of uracil residues (see **3b**,**c**). Phosphoramidites were synthesized after protection of **2b** with the isobutyryl residue and of **2c** with the benzoyl group. Duplexes containing the residues **2b** or **2c** gave always higher $T_m$ values than those of the nonmodified counterparts containing 2′-deoxyadenosine, the purine-2,6-diamine 2′-deoxyribonucleoside (**1**), or **2a** at the same positions. Six **2b** residues replacing dA in the duplex 5′-d(TAGGTCAATACT)-3′ (**11**)·5′-d(AGTATTGACCTA)-3′ (**12**) raised the $T_m$ value from 48 to 75° (4.5° per modification (*Table 3*)). Contrary to this, incorporation of the 5-halogenated 2′-deoxyuridines **3b** or **3c** into oligonucleotide duplexes showed very little influence on the thermal stability, regardless of which 'purine' nucleoside was located opposite to them (*Tables 4* and *5*). The positive effects on the thermal stability of duplexes observed in DNA were also found in DNA·RNA hybrids or in DNA with parallel chain orientation (*Tables 8* and *9*, resp.).

**Introduction.** – The thermal stability of oligonucleotide duplexes increases when 7-substituted 8-aza-7-deazapurines (= pyrazolo[3,4-*d*]pyrimidines) replace purines [1][2]. This effect is particularly strong when the heterocyclic base is an 8-aza-7-deazaguanine and carries a halogeno substituent at the 7-position [1][3][4]. Recent studies on the substitution of purine-2,6-diamine by the 7-bromo derivative of 8-aza-7-deazapurine-2,6-diamine have shown that this modified purine derivative forms as stable base a pair with thymine as guanine does with cytosine [5]. In contrast, the base pair of the structurally related purine-2,6-diamine 2′-deoxyribonucleoside (**1**; $n^2A_d$) with thymidine is rather weak when introduced into duplex DNA [5][6].

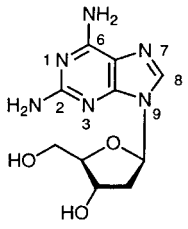


**1**

purine numbering

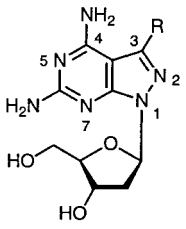


**2a** R = H
**b** R = Br
**c** R = I

systematic numbering

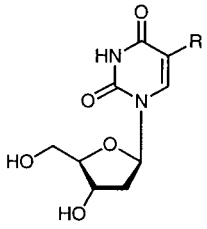


**3a** R = H
**b** R = Br
**c** R = I

This investigation compares the effects of halogeno substituents such as the bromo and iodo atom introduced at the 7-position of 8-aza-7-deazapurine-2,6-diamine 2′-deoxyribonucleosides (see **2b**,**c**) and at the 5-position of 2′-deoxyuridine (see **3b**,**c**) (purine numbering is used throughout the *General Part*; see **1**). These nucleosides are incorporated into various positions of duplex DNA, and the number of incorporations is increased stepwise. As the halogeno substituents are directed into the major groove, in both the 'purine'- and pyrimidine-nucleoside series, it is of interest to quantify the effects. Furthermore, the effect of multiple incorporations is investigated, as it is known from other duplex-stabilizing nucleosides that the stabilizing effects level off with an increasing number of modified nucleoside incorporations [7][8]. Oligonucleotide duplexes incorporating 7-halogenated 7-deazapurines (= pyrrolo[2,3-*d*]pyrimidines) show differences in the series of 7-iodo and 7-bromo compounds [9] that result from the spatial requirements of the halogeno substituent (*van der Waals* radii: Br = 1.85 Å; I = 1.98 Å [10]) and/or from the more hydrophobic character of the iodo substituents compared to the bromo residues. Thus, the 7-iodo derivative **2c** of the 8-aza-7-deazapurine-2,6-diamine nucleoside is synthesized and converted to a phosphoramidite, and a number of oligonucleotides are synthesized containing this 7-iodinated 8-aza-7-deazapurine-2,6-diamine nucleoside **2c**. A comparison of the thermal stability of these duplexes illustrates the striking differences in duplex stabilization among halogeno-substituted pyrimidine or 8-aza-7-deazapurine residues located in a similar environment of the major groove of B-DNA.

**Results and Discussion.** – 1. *Synthesis and Properties of Monomers.* The 7-iodinated 8-aza-7-deazapurine-2,6-diamine 2′-deoxyribonucleoside **2c** was prepared from the 6-isopropoxy compound **4** [11] upon treatment with 25% aqueous $NH_3$ solution at 70° for 4 days in an autoclave. The nucleosides **2a**,**b** [11] as well as the 2′-deoxyuridine derivatives **3a**–**c** have been described elsewhere [12]. The halogeno substituents change the mobility of the nucleosides on a reversed-phase HPLC column, with the iodinated **2c** and **3c** as the slowest migrating compounds (*Fig. 1*, *a* and *b*). The retention times refer to the hydrophobic character of the nucleosides; the data were used later for the composition analysis of the base-modified oligonucleotides.

The nucleobases of the modified nucleosides **2a**–**c** and **3a**–**c** influence the $N \leftrightarrow S$ pseudorotational equilibrium of the sugar moiety. This affects the conformation of the sugar-phosphate backbone of DNA. For this reason, the $^1$H-NMR spectra of the pyrazolo[3,4-*d*]pyrimidine nucleoside **2c** as well as of the pyrimidine nucleosides **3a**–**c** were measured in $D_2O$, and $^3J$(H,H) NMR coupling constants were determined. The conformational analysis was performed on the basis of these coupling constants with the program PSEUROT [13]. According to *Table 1*, the 8-aza-7-deazapurin-2,6-diamine nucleoside **2a** shows a higher *N*-conformer population than the corresponding purine nucleoside **1**. The conformation around the C(4′)–C(5′) bond indicates that the 8-aza-7-deazapurine-2,6-diamine nucleoside **2c**, as the 8-aza-7-deaza-2′-deoxyguanosines [14], prefers the $\gamma^t$-(−*sc*)-rotamer population, while, for the regular purine nucleosides, the $\gamma^{g+}$-(+*sc*)- or the $\gamma^{g-}$-(*ap*) conformation is predominant [15]. The conformation of the sugar moieties of the pyrimidine nucleosides **3a**–**c** is also influenced by the substitution at the 5-position (*Table 1*). The main change is observed

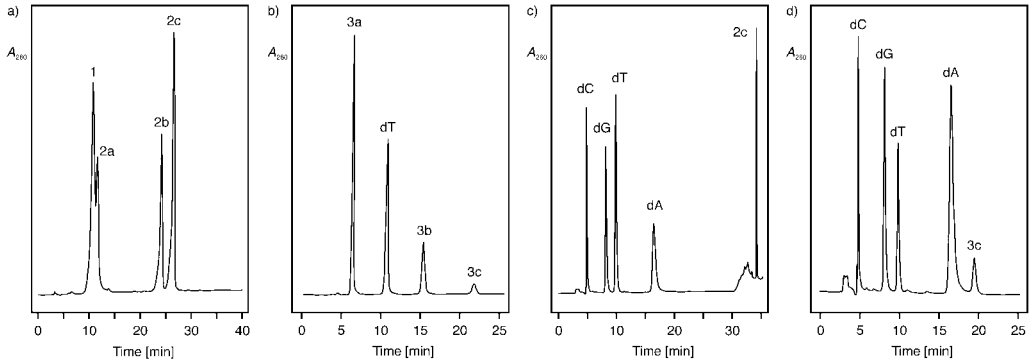


Fig. 1. *HPLC Profiles of* a) *the nucleosides* **1** *and* **2a**–**c** *and* b) *the nucleosides* **3a**–**c** *and* dT. c) d) *HPLC Profiles of the enzymatic-hydrolysis products of the oligonucleotides* **21** *and* **28**, *respectively, obtained by digestion with snake-venom phosphodiesterase followed by alkaline phosphatase in 0.1*M Tris·*HCl buffer* (pH 8.3) *at 37°*. The nucleoside mixtures were analyzed by reversed-phase HPLC at 260 nm on a *RP-18* column (200 × 10 mm). Gradient for *a*): 0–50 min *B* in *A* (0%–100%), for *b*) and *d*): 0–30 min 100% *A*; for *c*) 0–20 min 100% *A*, 20–50 min *B* in *A* (0% → 100%), 0.7 ml/min (*A* = buffer (see *Exper. Part*), *B* = MeCN).

Table 1. *$^3$J(H,H) Coupling Constants of the Sugar Moieties and* N/S-*Conformer Populations of the 2′-Deoxyribonucleosides* **1**–**3** *at 303 K*[a])

| | $^3J$(H,H)/Hz | | | | | | | Conformation | | | | |
|---|---|---|---|---|---|---|---|---|---|---|---|---|
| | $J(1',2')$ | $J(1',2'')$ | $J(2',3')$ | $J(2'',3')$ | $J(3',4')$ | $J(4',5')$ | $J(4',5'')$ | %*N* | %*S* | $\gamma^{g^+}$ | $\gamma^{t}$ | $\gamma^{g^-}$ |
| **1** | 7.30 | 6.10 | 7.00 | 3.10 | 3.40 | 3.20 | 4.30 | 31 | 69 | 62 | 25 | 13 |
| **2a** | 6.60 | 6.80 | 6.90 | 3.70 | 3.60 | 4.00 | 5.80 | 37 | 63 | 36 | 42 | 22 |
| **2c** | 6.60 | 6.70 | 6.85 | 3.90 | 3.85 | 4.30 | 5.90 | 38 | 62 | 31 | 43 | 26 |
| **dT** [16] | – | – | – | – | – | – | – | 36 | 64 | – | – | – |
| **3a** | 6.70 | 6.60 | 6.50 | 4.30 | 4.10 | 3.60 | 5.20 | 30 | 70 | 47 | 35 | 18 |
| **3b** | 6.45 | 6.50 | 6.50 | 4.70 | 4.50 | 3.40 | 4.70 | 34 | 66 | 55 | 30 | 15 |
| **3c** | 6.50 | 6.50 | 6.50 | 4.50 | 4.40 | 3.40 | 4.80 | 33 | 67 | 54 | 31 | 15 |

[a]) Solvent $D_2O$; r.m.s. < 0.4 Hz; $|\Delta J_{max}|$ < 0.4 Hz.

between **3a** without a 5-substituent and the derivatives dT or **3b**,**c** with a Me or halogeno substituent.

As the reactivities of the amino groups of the nucleoside **2b** are rather different from those of **1**, various residues were studied for the base protection. Earlier, nucleoside **2b** was protected with the *N*,*N*-dibutylformamidine (dnb) residue. Now, the isobutyryl (ibu) group was introduced by the protocol of transient protection (**2b** → **5a**) [17] (*Scheme*). As a by-product, the monoprotected nucleoside **6** was isolated (22%). The formation of mono-acylated compounds has been observed in the case of other purine-2,6-diamine nucleosides [18]. When performing the alkaline hydrolysis of compounds **5a** or **6** in 25% aqueous $NH_3$ solution at 40°, a fast deprotection was observed. The half-life for **5a** and **6** were determined and found to be 4.5 and 20.5 min, respectively, indicating that this protecting group is appropriate for the solid-phase oligonucleotide synthesis. For the protection of the iodo nucleoside **2c**, the transient

*Scheme*

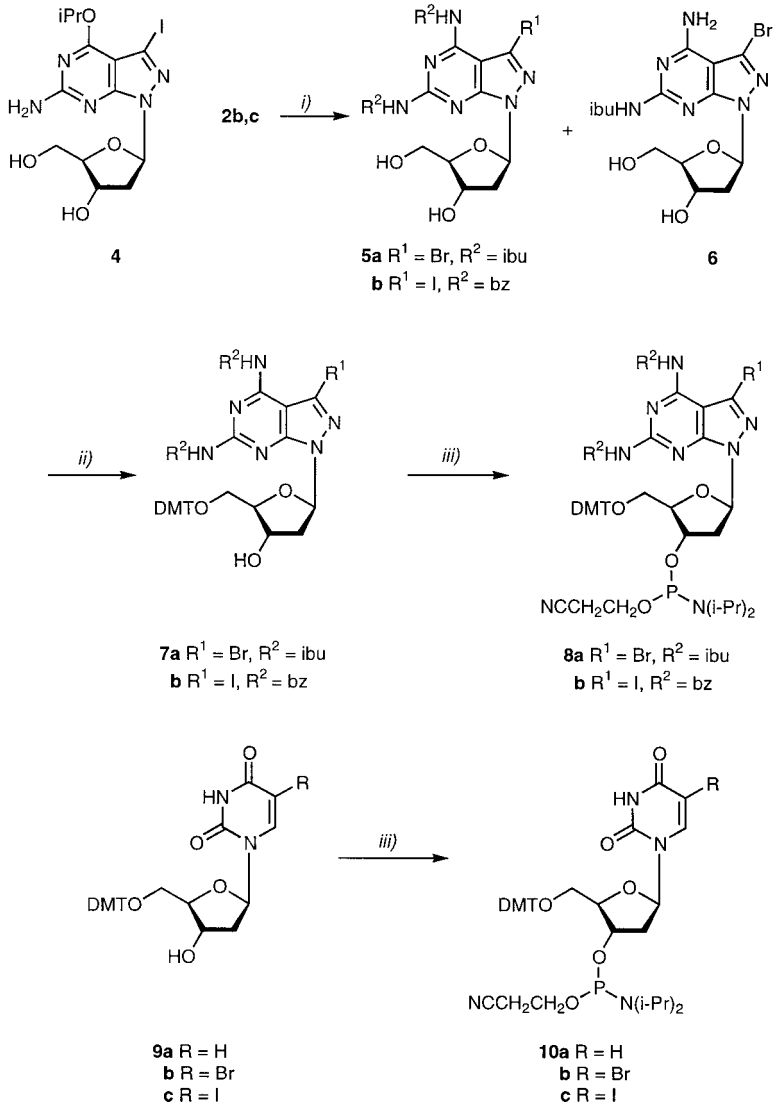


*i*) **5a**: **2b**, $Me_3SiCl$, pyridine, isobutyric anhydride, r.t., 4 h; **5b**: **2c**, $Me_3SiCl$, pyridine, benzoyl chloride, r.t., 24 h. *ii*) $(MeO)_2TrCl$, pyridine, r.t., 4 h. *iii*) 2-Cyanoethyl diisopropylphosphoramidochloridite, $CH_2Cl_2$ (for **8b** in THF), r.t., 30 min.

protection protocol was used as in **2b**, but in this case, a benzoyl group was chosen (**2c** → **5b**). The time for complete deprotection of **5b** (25% aqueous $NH_3$ solution, 40°, HPLC monitoring at 260 nm) was 450 min. A half-life was not determined because of the stepwise nature of the reaction.

The base-protected nucleosides **5a**,**b** as well as the pyrimidine nucleosides **3a**–**c** were converted to the $(MeO)_2Tr$ derivatives **7a**,**b**, and **9a**–**c** under standard reaction conditions [19]. Phosphitylation of the $(MeO)_2Tr$ derivatives **7a**,**b** was performed in $CH_2Cl_2$ or THF in the presence of 2-cyanoethyl diisopropylphosphoramidochloridite to furnish the phosphoramidites **8a**,**b** (*Scheme*); the pyrimidine building blocks **10a**–**c** were prepared from **9a**–**c** in $CH_2Cl_2$ [19]. The phosphoramidites **8a**,**b** and **10a**–**c** were then employed in solid-phase oligonucleotide synthesis. All compounds were characterized by $^1$H-, $^{13}$C-, and $^{31}$P-NMR spectra and by elemental analysis (*Table 2* and *Exper. Part*). *Table 2* summarizes the $^{13}$C-NMR data of 8-aza-7-deazapurine as well

Table 2. *$^{13}$C-NMR Chemical Shifts of Pyrazolo[3,4-*d*]pyrimidine-4,6-diamine 2′-Deoxyribonucleosides*[a])

| | C(2)[b]) C(6)[c]) | C(4)[b]) C(7)[c]) | C(5)[b]) C(3°)[c]) | C(6)[b])[d]) C(4)[c]) | C(7)[c]) C(3)[c]) | C=O/=CH | C=O/=CH | C(1′) | C(2′) | C(3′) | C(4′) | C(5′) |
|---|---|---|---|---|---|---|---|---|---|---|---|---|
| **2b** | 157.6 | 157.4 | 94.5 | 162.7 | 119.2 | | | 83.0 | 37.5 | 70.9 | 87.3 | 62.4 |
| **2c** | 157.0 | 157.6 | 91.2 | 162.2 | 98.3 | | | 83.1 | 37.6 | 70.9 | 87.3 | 62.4 |
| **3a** | 163.2 | 150.5 | 101.8 | 140.6 | | | | 84.2 | 38.5 | 70.5 | 87.4 | 61.3 |
| **3b** | 159.1 | 149.7 | 95.6 | 140.6 | | | | 84.7 | 38.4 | 69.9 | 87.5 | 60.7 |
| **3c** | 160.4 | 150.0 | 69.9 | 145.0 | | | | 84.6 | [e]) | 69.2 | 87.4 | 60.7 |
| **5a** | 155.8 | 153.8 | 104.7 | 156.2 | 121.4 | 175.2 | 176.5 | 83.6 | 37.5 | 70.7 | 87.7 | 62.2 |
| **5b** | 149.6 | 152.1 | 105.7 | 153.4 | 96.3 | 169.4 | 177.5 | 84.4 | 38.7 | 71.6 | 88.6 | 63.1 |
| **6** | 156.0 | 156.5 | 97.4 | 157.5 | 119.1 | 175.3 | | 83.3 | 37.5 | 70.8 | 87.5 | 62.2 |
| **7a** | 155.6 | 154.9 | 98.5 | 157.5 | 117.2 | 174.7 | 175.2 | 83.5 | 37.6 | 72.2 | 85.4 | 63.6 |
| **7b** | 149.5 | 152.1 | 105.8 | 153.2 | 96.2 | – | 177.5 | 84.8 | [e]) | 71.6 | 86.7 | 65.3 |
| **9a** | 163.0 | 158.0 | 101.5 | 144.7 | | | | 84.1 | [e]) | 69.9 | 85.3 | 63.4 |
| **9b** | 158.0 | 159.1 | 96.0 | 144.7 | | | | 84.9 | 38.4 | 70.3 | 85.7 | 63.6 |
| **9c** | 158.0 | 160.5 | 69.8 | 144.2 | | | | 84.8 | 38.4 | 70.4 | 85.8 | 63.7 |

[a]) Measured in $(D_6)$DMSO at 303 K. [b]) Purine numbering. [c]) Systematic numbering. [d]) Tentative. [e]) Superimposed by $(D_6)$DMSO.

as those of pyrimidine nucleosides. The assignment was made according to gated-decoupled spectra. The NMR data of **3a**–**c** were included, as a literature search gave little information on that matter.

2. *Oligonucleotides.* 2.1. *Synthesis and Characterization*. Automated solid-phase synthesis of the oligonucleotides (**11**–**37**, *Tables 3–9*) was performed with the phosphoramidites **8a**,**b** and **10a**–**c** as well as the standard building blocks. The syntheses followed the standard protocol [20], and the coupling yields were always higher than 97%. Oligonucleotides containing halogenated dU residues require the use of the [4-(*tert*-butyl)phenoxy]acetyl (tac) group for the protection of the canonical phosphoramidites [21]. In these cases, the deprotection was performed with conc. ammonia at room temperature, while in all other cases, the deprotection was carried out at 60°. The oligonucleotides were detritylated and purified on purification cartridges [22] or by reversed-phase HPLC (conditions for purification, see *Exper. Part*). The homogeneity of the compounds was established by ion-exchange chromatography (see *Exper. Part*). The composition of the oligonucleotides was determined by tandem hydrolysis with snake-venom phosphodiesterase and alkaline phosphatase followed by reversed-phase (*RP-18*) HPLC as described [23]. Typical examples are

shown in *Fig. 1,c* and *d*. The newly incorporated iodonucleosides **2c** or **3c** migrate slower than the canonical DNA constituents. The oligonucleotides were also characterized by MALDI-TOF mass spectra. The detected masses were in good agreement with the calculated values (see *Exper. Part*, *Table 10*).

2.2. *Base-Pair Stabilities of the Oligonucleotide Duplexes.* Previously, the 7-bromo nucleoside **2b** was found to stabilize DNA duplexes strongly, while the non-halogenated compound **2a** contributes very little to the duplex stability [1][5]. The contribution of the purine-2,6-diamine nucleoside **1** to the duplex stability is even lower [6][24]. Thus, DNA duplexes containing **1** · thymidine base pairs are only slightly more stable than those with dA · dT pairs. As it was not known whether the stabilizing effect of the bromo nucleoside **2b** would increase continuously with an increasing number of incorporations or would level off with multiple incorporations – as it is reported for other modified nucleosides [7] – a series of oligonucleotides were synthesized that contain the halogenated compound **2b** in a consecutive manner or in distant position. The modified residues were incorporated in one or both strands of a double-stranded DNA. The total number of incorporations was increased in duplexes from 1 to 6. The non-halogenated duplexes containing compound **2a** were prepared for comparison. Apart from the incorporation of the bromo nucleoside **2b**, the iodo compound **2c** was also studied. For all experiments, the non-self-complementary duplex 5′-d(TAGGT-CAATACT)-3′ (**11**) · 5′-d(AGTATTGACCTA)-3′ (**12**) was chosen.

The nonhalogenated nucleoside **2a** increases the $T_m$ value of the standard duplex **11** · **12** by only 1.5° per modified residue (*Table 3* and [5]). Contrarily, the bromo compound **2b** contributes a 4–5° stabilization per modified residue, which represents an outstandingly high value induced by a non-canonical base. The strength of this effect is sequence-dependent, but the stability of the duplexes increases with an increasing number of **2b** incorporations, as shown in *Fig. 2*. When the iodo nucleoside **2c** replaces

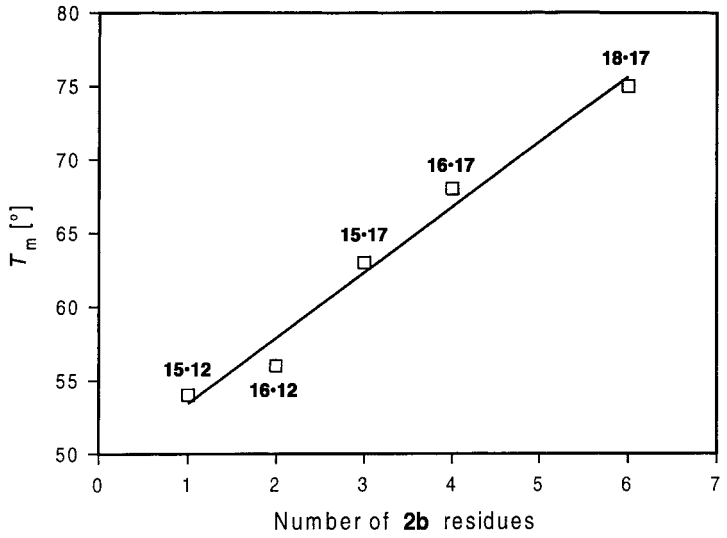


Fig. 2. *Graph of the* $T_m$ *values against the number of* **2b** *residues*

Table 3. $T_m$ *Values and Thermodynamic Data of Duplex Formation of Oligonucleotides Containing the Pyrazolo[3,4-*d*]pyrimidine Nucleosides* **2a**–**c** *Opposite to dT*[a])

| | $T_m$ [°C] | $\Delta H^\circ$ [kcal/mol] | $\Delta S^\circ$ [kcal/mol K] | $\Delta G^\circ_{310}$ [kcal/mol] |
|---|---|---|---|---|
| 5′-d(TAG GTC AAT ACT)-3′ (**11**)<br>3′-d(ATC CAG TTA TGA)-5′ (**12**) | 47 | – 83.8 | – 235.9 | – 10.6 |
| 5′-d(TAG GTC **2a2a**T ACT)-3′ (**13**)<br>3′-d(ATC CAG TTA TGA)-5′ (**12**) | 50 | – 93.3 | – 263.09 | – 11.7 |
| 5′-d(TAG GTC AAT ACT)-3′ (**11**)<br>3′-d(ATC C**2a**G TT**2a** TGA)-5′ (**14**) | 50 | – 98.79 | – 279.63 | – 12.06 |
| 5′-d(TAG GTC **2a2a**T ACT)-3′ (**13**)<br>3′-d(ATC C**2a**G TT**2a** TGA)-**5**′ (**14**) | 51 | – 98.66 | – 278.58 | – 12.26 |
| 5′-d(TAG GTC **2b**AT ACT)-3′ (**15**)<br>3′-d(ATC CAG TTA TGA)-5′ (**12**) | 54 | – 99.96 | – 280.74 | – 12.89 |
| 5′-d(TAG GTC **2b2b**T ACT)-3′ (**16**)<br>3′-d(ATC CAG TTA TGA)-5′ (**12**) | 56 | – 91.42 | – 251.66 | – 13.37 |
| 5′-d(TAG GTC AAT ACT)-3′ (**11**)<br>3′-d(ATC C**2b**G TT**2b** TGA)-5′ (**17**) | 59 | – 91.85 | – 251.25 | – 13.92 |
| 5′-d(TAG GTC **2b**AT ACT)-3′ (**15**)<br>3′-d(ATC C**2b**G TT**2b** TGA)-5′ (**17**) | 63 | – 100.70 | – 274.04 | – 15.70 |
| 5′-d(TAG GTC **2b2b**T ACT)-3′ (**16**)<br>3′-d(ATC C**2b**G TT**2b** TGA)-5′ (**17**) | 67 | – 105.40 | – 285.02 | – 17.00 |
| 5′-d(T**2b**G GTC **2b2b**T **2b**CT)-3′ (**18**)<br>3′-d(ATC CAG TTA TGA)-5 (**12**) | 64 | – 99.08 | – 268.47 | – 15.81 |
| 5′-d(T**2b**G GTC **2b2b**T **2b**CT)-3′ (**18**)<br>3′-d(ATC C**2b**G TT**2b** TGA)-5′ (**17**) | 75 | – 107.43 | – 283.41 | – 19.53 |
| 5′-d(TAG GTC AAT ACT)-3′ (**11**)<br>3′-d(ATC C**2c**G TTA TGA)-5′ (**19**) | 51 | – 90.65 | – 254.58 | – 11.69 |
| 5′-d(TAG GTC AAT ACT)-3′ (**11**)<br>3′-d(ATC CAG TT**2c** TGA)-5′ (**20**) | 54 | – 93.22 | – 260.43 | – 12.45 |
| 5′-d(TAG GTC AAT ACT)-3′ (**11**)<br>3′-d(ATC C**2c**G TT**2c** TGA)-5′ (**21**) | 57 | – 95.09 | – 263.29 | – 13.43 |
| 5′-d(TAG GTC **2c2c**T ACT)-3′ (**22**)<br>3′-d(ATC CAG TTA TGA)-5′ (**11**) | 55 | – 96.46 | – 268.72 | – 13.12 |
| 5′-d(TAG GTC **2c2c**T ACT)-3′ (**22**)<br>3′-d(ATC C**2c**GT T A TGA)-5′ (**19**) | 59 | – 102.95 | – 284.63 | – 14.67 |
| 5′-d(TAG GTC **2c2c**T ACT)-3′ (**22**)<br>3′-d(ATC C**2c**GT T**2c** TGA)-5′ (**21**) | 66 | – 104.93 | – 284.73 | – 16.62 |
| 5′-d(T**2c**G GTC**2c2c**T **2c**CT)-3′ (**23**)<br>3′-d(ATC C**2c**G TT**2c** TGA)-5′ (**21**) | 72 | – | – | – |

[a]) Thermodynamic parameters are derived from the fitting of melting curves measured at 260 nm in 0.1M NaCl, 10 mM $MgCl_2$, and 10 mM Na-cacodylate buffer, pH 7.0, with 5 μM + 5 μM single-strand concentration. The $\Delta G^\circ$ are taken directly from the program Meltwin 3.0 referring to 310°. Earlier reports from our laboratory obtained with the fitting program refer to the same temperature and not to 298° as indicated. The thermodynamic data determined by the *van't Hoff* plots from the concentration dependence of the $T_m$ values are consistent within 15% with those obtained from the curve fitting. The *van't Hoff* data of the formation of the duplex **11**·**12** are the following: $\Delta H^\circ = -86.8$ kcal/mol; $\Delta S^\circ = -243.7$ cal/mol K; $\Delta G^\circ_{310} = -11.3$ kcal/mol.

the bromo compound **2b**, a similar effect regarding duplex stabilization is observed (*Table 3*). The effects of halogeno substituents introduced into the pyrazolo-[3,4-*d*]pyrimidine derivatives of dG [3] or dA [2] amounts only to 2° per modified residue.

A similar set of experiments as described for the duplexes containing the halogenated 8-aza-7-deazapurine nucleosides **2b** or **2c** were performed with the halogenated 2′-deoxyuridine derivatives **3b** or **3c** (*Table 4*). Neither the bromo nucleoside **3b** nor the iodo nucleoside **3c** increases the stability of the duplexes significantly compared to that of the nonhalogenated **3a** or dT. Thus, only the base pairs of type **I** (*Fig. 3,a*) with halogeno substituents located at the 7-position of the

Table 4. $T_m$ *Values and Thermodynamic Data of Duplex Formation of Oligonucleotides Containing the Pyrimidine Nucleosides* **3a**–**c** *Opposite to dA*[a])

| | $T_m$ [°C] | $\Delta H°$ [kcal/mol] | $\Delta S°$ [cal/mol K] | $\Delta G°_{310}$ [kcal/mol] |
|---|---|---|---|---|
| 5′-d(TAG G**3a**C AA**3a** ACT)-3′ (**24**)<br>3′-d(ATC CAG TTA TGA)-5′ (**12**) | 47 | – 86.35 | – 244.74 | – 10.45 |
| 5′-d(TAG GTC AAT ACT)-3′ (**11**)<br>3′-d(ATC CAG **3a3a**A TGA)-5′ (**25**) | 48 | – 92.11 | – 261.95 | – 10.86 |
| 5′-d(TAG G**3a**C AA**3a** ACT)-3′ (**24**)<br>3′-d(ATC CAG **3a3a**A TGA)-5′ (**25**) | 46 | – 86.37 | – 245.42 | – 10.25 |
| 5′-d(TAG G**3b**C AA**3b** ACT)-3′ (**26**)<br>3′-d(ATC CAG TTA TGA)-5′ (**12**) | 48 | – 95.76 | – 271.88 | – 11.44 |
| 5′-d(TAG GTC AAT ACT)-3′ (**11**)<br>3′-d(ATC CAG **3b3b**A TGA)-5′ (**27**) | 49 | – 97.43 | – 276.95 | – 11.53 |
| 5′-d(TAG G**3b**C AA**3b** ACT)-3′ (**26**)<br>3′-d(ATC CAG **3b3b**A TGA)-5′ (**27**) | 49 | – 94.25 | – 267.57 | – 11.26 |
| 5′-d(TAG G**3c**C AA**3c** ACT)-3′ (**28**)<br>3′-d(ATC CAG TTA TGA)-5′ (**12**) | 49 | – 96.38 | – 273.73 | – 11.48 |
| 5′-d(TAG GTC AAT ACT)-3′ (**11**)<br>3′-d(ATC CAG **3c3c**A TGA)-5′ (**29**) | 50 | – 94.99 | – 269.20 | – 11.50 |
| 5′-d(TAG G**3c**C AA**3c** ACT)-3′ (**28**)<br>3′-d(ATC CAG **3c3c**A TGA)-5′ (**29**) | 50 | – 99.14 | – 281.47 | – 11.85 |

[a]) See *Table 3*.

8-aza-7-deazapurine (pyrazolo[3,4-*d*]pyrimidine) moiety are stabilized by the halogeno substituents, while those of type **II** (*Fig. 3,a*) with the halogeno atoms attached at the 5-positions of the pyrimidine base exert little influence compared to those with dA · dT pairs.

As the stability of the base pairs of the halogenated pyrimidine nucleosides **3b** or **3c** with dA was low compared to the halogenated pyrazolo[3,4-*d*]pyrimidine compounds **2b** or **2c** incorporated opposite to dT, tridentate base pairs are formed in which the halogenated pyrimidine nucleosides **3a**–**c** are located opposite to the purine-2,6-diamine nucleoside **1** instead of dA (*Fig. 3,b*; base-pair type **III**). In this case, a strengthening of the base pair can be expected if the formation of a third H-bond is

possible. However, the $T_m$ values of those duplexes were also not influenced significantly by replacement of the dA residues by the nucleoside **1** (*Table 5*). This indicates that the 2-amino group does not participate in possible base pairs as shown in **IIIa**–**c** (*Fig. 3*,*b*), a finding similar to that observed for a base pair between **1** and dT [5][6][24]. Similar behavior was found in the case of duplexes containing the base pair **IVa** (*Fig. 3*,*b*) formed between nucleoside **2a** and the pyrimidine nucleosides **3a**–**c** (*Table 5*). Nevertheless, the duplexes incorporating the base pairs **IVb**,**c** are slightly more stable than those containing the base pairs **IIIb**,**c**.

Significant duplex stabilization was observed when the halogenated 8-aza-7-deazapurine nucleosides **2b** or **2c** were incorporated opposite to the pyrimidine

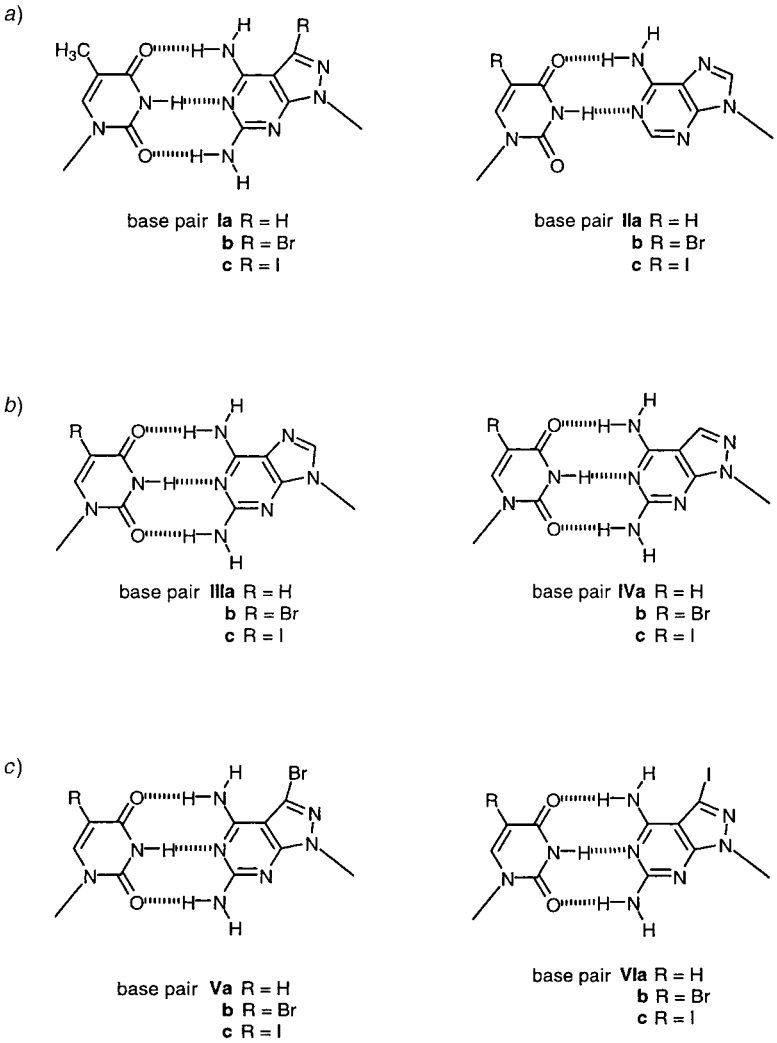


Fig. 3. *Base-pair types* **I**–**VI**

Table 5. $T_m$ *Values and Thermodynamic Data of Oligonucleotide Duplexes Containing the Halogenated Pyrimidine Nucleosides* **3a–c** *Opposite to the Purine-2,6-diamine Nucleoside* **1** *or the Pyrazolo[3,4-d]pyrimidine-4,6-diamine Nucleoside* **2a**[a])

| | $T_m$ [°C] | $\Delta H^\circ$ [kcal/mol] | $\Delta S^\circ$ [cal/mol K] | $\Delta G^\circ_{310}$ [kcal/mol] |
|---|---|---|---|---|
| 5′-d(TAG GTC AAT ACT)-3′ (**11**)<br>3′-d(ATC C**1**G TT**1** TGA)-5′ (**30**) | 49 | – 83.15 | – 232.81 | – 10.94 |
| 5′-d(TAG G**3a**C AA**3a** ACT)-3′ (**24**)<br>3′-d(ATC C**1**G TT**1** TGA)-5′ (**30**) | 48 | – 73.03 | – 202.44 | – 10.25 |
| 5′-d(TAG G**3b**C AA**3b** ACT)-3′ (**26**)<br>3′-d(ATC C**1**G TT**1** TGA)-5′ (**30**) | 49 | – 73.84 | – 203.94 | – 10.59 |
| 5′-d(TAG G**3c**C AA**3c** ACT)-3′ (**28**)<br>3′-d(ATC C**1**G TT**1** TGA)-5′ (**30**) | 49 | – 77.60 | – 215.48 | – 10.76 |
| 5′-d(T**1**G GTC **11**T **1**CT)-3′ (**31**)<br>3′-d(ATC CAG TTA TGA)-5′ (**12**) | 48 | – 54.74 | – 144.65 | – 9.88 |
| 5′-d(T**1**G GTC **11**T **1**CT)-3′ (**31**)<br>3′-d(ATC CAG **3a3a**A TGA)-5′ (**25**) | 48 | – 60.03 | – 161.49 | – 9.94 |
| 5′-d(T**1**G GTC **11**T **1**CT)-3′ (**31**)<br>3′-d(ATC CAG **3b3b**A TGA)-5′ (**27**) | 48 | – 60.09 | – 160.37 | – 10.35 |
| 5′-d(T**1**G GTC **11**T **1**CT)-3′ (**31**)<br>3′-d(ATC CAG **3c3c**A TGA)-5′ (**29**) | 48 | – 62.35 | – 167.33 | – 10.45 |
| 5′-d(TAG GTC **2a2a**T ACT)-3′ (**13**)<br>3′-d(ATC CAG **3a3a**A TGA)-5′ (**25**) | 49 | – 87.32 | – 245.54 | – 11.16 |
| 5′-d(TAG GTC **2a2a**T ACT)-3′ (**13**)<br>3′-d(ATC CAG **3b3b**A TGA)-5′ (**27**) | 50 | – 89.11 | – 250.34 | – 11.47 |
| 5′-d(TAG GTC **2a2a**T ACT)-3′ (**13**)<br>3′-d(ATC CAG **3c3c**A TGA)-5′ (**29**) | 51 | – 81.32 | – 225.60 | – 11.35 |
| 5′-d(TAG G**3a**C AA**3a** ACT)-3′ (**24**)<br>3′-d(ATC C**2a**G TT**2a** TGA)-5′ (**14**) | 49 | – 90.30 | – 253.96 | – 11.53 |
| 5′-d(TAG G**3b**C AA**3b** ACT)-3′ (**26**)<br>3′-d(ATC C**2a**G TT**2a** TGA)-5′ (**14**) | 51 | – 93.05 | – 261.91 | – 11.82 |
| 5′-d(TAG G**3c**C AA**3c** ACT)-3′ (**28**)<br>3′-d(ATC C**2a**G TT**2a** TGA)-5′ (**14**) | 50 | – 90.58 | – 254.11 | – 11.77 |

[a]) See *Table 3*.

nucleosides **3a–c** (*Table 6* and *Fig. 3,c*; base-pair type **V** and **VI**). The $T_m$ increase amounts to *ca.* 4–5° per incorporated residue of the halogenated nucleosides **2b** or **2c**. All duplexes containing the halogenated nucleosides **2b** or **2c** (*Fig. 3,c*) give very similar $T_m$ values, no matter which pyrimidine monomer is located opposite to it. Thus, only halogeno substituents attached at the modified purine residues lead to a duplex stabilization, while halogeno atoms at the 5-position of the 2′-deoxyuridine moiety contribute very little to the duplex stability [25][26].

2.3. *Base Discrimination*. – To investigate the discrimination of the iodo nucleoside **2c** towards the four canonical DNA constituents, hybridization experiments were performed according to *Table 7*. As expected, the base pair **2c**·dT is the strongest (**11**·**21**, $T_m$ 57°), while those of the duplexes forming mismatches melt at a significantly

Table 6. $T_m$ *Values and Thermodynamic Data of Oligonucleotides Containing the Pyrazolo[3,4-*d*]pyrimidine-4,6-diamine Nucleosides* **2b**,**c** *Opposite to dT and* **3a**–**c**[a])

| | $T_m$ [°C] | $\Delta H^\circ$ [kcal/mol] | $\Delta S^\circ$ [cal/mol K] | $\Delta G^\circ_{310}$ [kcal/mol] |
|---|---|---|---|---|
| 5′-d(TAG GTC **2b**AT ACT)-3′ (**15**)<br>3′-d(ATC CAG **3a3a**A TGA)-5′ (**25**) | 52 | – 92.88 | – 260.97 | – 11.94 |
| 5′-d(TAG GTC **2b2b**T ACT)-3′ (**16**)<br>3′-d(ATC CAG **3a3a**A TGA)-5′ (**25**) | 55 | – 96.78 | – 269.67 | – 13.14 |
| 5′-d(T**2b**G GTC **2b2b**T **2b**CT)-3′ (**18**)<br>3′-d(ATC CAG **3a3a**A TGA)-5′ (**25**) | 64 | – 101.57 | – 276.51 | – 15.82 |
| 5′-d(TAG GTC **2b**AT ACT)-3′ (**15**)<br>3′-d(ATC CAG **3b3b**A TGA)-5′ (**27**) | 54 | – 98.06 | – 275.03 | – 12.76 |
| 5′-d(TAG GTC **2b2b**T ACT)-3′ (**16**)<br>3′-d(ATC CAG **3b3b**A TGA)-5′ (**27**) | 55 | – 95.42 | – 266.68 | – 12.71 |
| 5′-d(T**2b**G GTC **2b2b**T **2b**CT)-3′ (**18**)<br>3′-d(ATC CAG **3b3b**A TGA)-5′ (**27**) | 65 | – 106.49 | – 290.34 | – 16.44 |
| 5′-d(TAG GTC **2b**AT ACT)-3′ (**15**)<br>3′-d(ATC CAG **3c3c**A TGA)-5′ (**29**) | 54 | – 87.97 | – 244.29 | – 12.20 |
| 5′-d(TAG GTC **2b2b**T ACT)-3′ (**16**)<br>3′-d(ATC CAG **3c3c**A TGA)-5′ (**29**) | 55 | – 89.17 | – 246.44 | – 12.74 |
| 5′-d(T**2b**G GTC **2b2b**T **2b**CT)-3′ (**18**)<br>3′-d(ATC CAG **3c3c**A TGA)-5′ (**29**) | 65 | – 101.57 | – 275.34 | – 16.18 |
| 5′-d(TAG G**3a**C AA**3a** ACT)-3′ (**24**)<br>3′-d(ATC C**2b**G TT**2b** TGA)-5′ (**17**) | 56 | – 95.76 | – 265.45 | – 13.43 |
| 5′-d(TAG G**3b**C AA**3b** ACT)-3′ (**26**)<br>3′-d(ATC C**2b**G TT**2b** TGA)-5′ (**17**) | 56 | – 96.53 | – 268.70 | – 13.20 |
| 5′-d(TAG G**3c**C AA**3c** ACT)-3′ (**28**)<br>3′-d(ATC C**2b**G TT**2b** TGA)-5′ (**17**) | 57 | – 97.07 | – 269.07 | – 13.62 |
| 5′-d(TAG G**3a**C AA**3a** ACT)-3′ (**24**)<br>3′-d(ATC C**2c**G TT**2c** TGA)-5′ (**21**) | 55 | – 96.93 | – 270.69 | – 12.98 |
| 5′-d(TAG G**3b**C AA**3b** ACT)-3′ (**26**)<br>3′-d(ATC C**2c**G TT**2c** TGA)-5′ (**21**) | 55 | – 100.82 | – 282.19 | – 13.29 |
| 5′-d(TAG G**3c**C AA**3c** ACT)-3′ (**28**)<br>3′-d(ATC C**2c**G TT**2c** TGA)-5′ (**21**) | 55 | – 98.00 | – 273.26 | – 13.25 |

[a]) See *Table 3*.

lower temperature (*Table 7*). The discrimination of the iodo nucleoside **2c** is similar to that of the canonical nucleosides, except that the duplex **33**·**21** ($T_m$ 50°) shows a 7° lower $T_m$ value than the duplex **11**·**21** ($T_m$ 57°), while duplex **33**·**12** ($T_m$ 46°) has almost the same stability as the parent duplex **11**·**12** ($T_m$ 48°). The high $T_m$ value of **33**·**12** is the result of the formation of the dG·dA *Hoogsteen* pair, which is obviously not formed between dG and compound **2c**.

The CD spectra of the duplexes containing the 8-aza-7-deazaadenin-2-amine derivatives **2a**,**b** were measured next. A B-like DNA structure can be deduced from the curves displayed in *Fig. 4*,*a*. A positive *Cotton* effect around 270 to 290 nm and a negative lobe at 250 nm are observed for the standard duplex **11**·**12**. The CD spectrum

Table 7. $T_m$ *Values of Oligonucleotides Containing the Pyrazolo[3,4-*d*]pyrimidine-4,6-diamine Nucleoside* **2c** *Opposite to the Four Canonical Nucleosides*[a])

| | $T_m$ [°C] | | $T_m$ [°C] |
|---|---|---|---|
| 5′-d(TAG G**T**C AAT ACT)-3′ (**11**)<br>3′-d(ATC C**2c**G TT**2c** TGA)-5′ (**21**) | 57 | 5′-d(TAG G**T**C AAT ACT)-3′ (**11**)<br>3′-d(ATC C**A**G TTA TGA)-5′ (**12**) | 48 |
| 5′-d(TAG G**A**C AAT ACT)-3′ (**32**)<br>3′-d(ATC C**2c**G TT**2c** TGA)-5′ (**21**) | 45 | 5′-d(TAG G**A**C AAT ACT)-3′ (**32**)<br>3′-d(ATC C**A**G TTA TGA)-5′ (**12**) | 38 |
| 5′-d(TAG G**G**C AAT ACT)-3′ (**33**)<br>3′-d(ATC C**2c**G TT**2c** TGA)-5′ (**21**) | 50 | 5′-d(TAG G**G**C AAT ACT)-3′ (**33**)<br>3′-d(ATC C**A**G TTA TGA)-5′ (**12**) | 46 |
| 5′-d(TAG G**C**C AATACT)-3′ (**34**)<br>3′-d(ATC C**2c**G TT**2c** TGA)-5′ (**21**) | 45 | 5′-d(TAG G**C**C AATACT)-3′ (**34**)<br>3′-d(ATC C**A**G TTA TGA)-5′ (**12**) | 36 |

[a]) See *Table 3*.

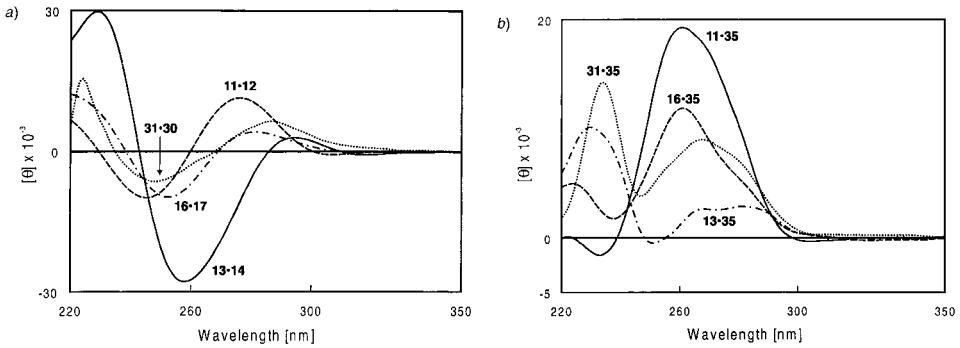


Fig. 4. a) *CD Spectra of duplexes* **11**·**12**, **13**·**14**, **16**·**17**, *and* **31**·**30** (in 100 mM NaCl, 10 mM $MgCl_2$, and 60 mM Na-cacodylate (pH 7.0)). b) *CD Spectra of duplexes* **11**·**35**, **13**·**35**, **16**·**35**, and **31**·**35** (in 100 mM NaCl, 10 mM $MgCl_2$, and 60 mM Na-cacodylate (pH 7.0)). Concentration of the oligonucleotides: 5 μM + 5 μM (single-strand concentration).

of the duplex **31**·**30** containing **1** shows significant differences similar to that of **16**·**17**, while the duplex **13**·**14** shows a stronger negative *Cotton* effect at 260 nm and a positive one at 235 nm. Similar differences were reported for the oligonucleotides containing 7-substituted 7-iodo-8-aza-7-deaza guanine [4].

2.4. *DNA-RNA Hybrids.* To study the influence of the 2,6-diamino-substituted nucleosides **1** and **2a**,**b** on the stability of DNA·RNA hybrids, the oligodeoxyribonucleotides **16**, **24**, **26**, **28**, **31**, and **11** were hybridized with the oligoribonucleotide **35**. *Table 8* shows that the various modifications exert a significant influence on the duplex stability of the DNA·RNA hybrids. While the incorporation of the nonhalogenated nucleosides **1** or **2a** stabilizes the DNA·RNA structure very little, the hybridization of the oligonucleotide containing **2b** with **35** (**16**·**35**) shows a significant increase of the duplex stability as in DNA. Compounds **3b** and **3c** enhance the thermal stability of DNA·RNA to a small degree, which is also observed for other modifications of 2′-deoxyuridine [27]. The hypochromicities of the chimeric hybrids are slightly decreased

Table 8. $T_m$ *Values and Thermodynamic Data of DNA · RNA Hybrids*[a])

| | $T_m$ [°C] | $\Delta H°$ [kcal/mol] | $\Delta S°$ [cal/mol K] | $\Delta G°_{310}$ [kcal/mol] |
|---|---|---|---|---|
| 5′-d(TAG GTC AAT ACT)-3′ (**11**)<br>3′-(AUC CAG UUA UGA)-5′ (**35**) | 45 | – 92.1 | – 264.0 | – 10.2 |
| 5′-d(T**1**G GTC **11**T **1**CT)-3′ (**31**)<br>3′-(AUC CAG UUA UGA)-5′ (**35**) | 48 | – 60.46 | – 162.12 | – 10.18 |
| 5′-d(TAG GTC **2a2a**T ACT)-3′ (**13**)<br>3′-(AUC CAG UUA UGA)-5′ (**35**) | 48 | – | – | – |
| 5′-d(TAG GTC **2b2b**T ACT)-3′ (**16**)<br>3′-(AUC CAG UUA UGA)-5′ (**35**) | 53 | – 98.64 | – 276.97 | – 12.74 |
| 5′-d(TAG GTC **2c2c**T ACT)-3′ (**22**)<br>3′-d(AUC CAG UUA UGA)-5′ (**35**) | 49 | – 84.55 | – 236.26 | – 11.28 |
| 5′-d(TAG G**3a**C AA**3a** ACT)-3′ (**24**)<br>3′-(AUC CAG UUA UGA)-5′ (**35**) | 44 | – 74.43 | – 208.26 | – 9.84 |
| 5′-d(TAG G**3b**C AA**3b** ACT)-3′ (**26**)<br>3′-(AUC CAG UUA UGA)-5′ (**35**) | 48 | – 77.19 | – 215.13 | – 10.47 |
| 5′-d(TAG G**3c**C AA**3c** ACT)-3′ (**28**)<br>3′-(AUC CAG UUA UGA)-5′ (**35**) | 47 | – 78.77 | – 220.52 | – 10.37 |

over those of the DNA · DNA duplexes (data not shown). From the CD spectra of *Fig. 3*, *b* it can be seen that the DNA · RNA hybrids adopt the A-form [28].

2.5. *Duplexes with Parallel Chain Orientation*. The base pairing of the nucleosides **1**, **2a** – **c** as well as **3b**,**c** was also investigated in parallel-stranded DNA [29]. For this purpose, it was necessary to replace the dC · dG pair by a $m^5iC_d \cdot iG_d$ pair. The duplexes **11** · **36** and **37** · **12** served as standards [29]. Substitution of dA residues by the diamino nucleoside **1** resulted in a slight stability decrease of the parallel-stranded (ps) duplexes **31** · **36** and **37** · **30** (*Table 9*). The incorporation of **2a** – **c** into the ps DNA resulted in a significant increase of the $T_m$ values. The incorporation of the substituted pyrimidine nucleosides **3b**,**c** in place of dT leads only to minor changes of the $T_m$ values. From this, it can be concluded that similar to DNA with antiparallel chain orientation, the halogeno substituents of the 'purine' nucleosides **2b**,**c** stabilize these duplexes, while the halogeno substituents of the pyrimidine nucleosides contribute very little to the duplex stability.

**Conclusion.** – The halogeno substituents introduced at the 7-position of the 8-aza-7-deazapurine 2′-deoxynucleoside (see **2b**,**c**) or the 5-position of 2′-deoxyuridine residues (see **3b**,**c**) have very different influences on the stability of nucleic acid duplexes. In the case of the 7-halogenated 8-aza-7-deazapurine 2′-deoxynucleosides **2b**,**c**, each monomer contributes *ca.* 4 – 5° to the duplex stabilization, while the pyrimidine nucleosides **3b**,**c** show very little influence or even no effect. This is surprising, as the halogeno atoms in both series of nucleobases are directed into the major groove of B-DNA, both being in a nonidentical but very similar environments. When both, the halogenated pyrimidines and the halogenated 8-aza-7-deazapurine nucleosides are present in a DNA duplex, only the latter make a contribution to the duplex stabilization. Consequently, the increase of the hydrophobic character of the major groove induced by the lipophilic halogeno substituents and the expelling of $H_2O$ molecules is not the major effect

Table 9. $T_m$ *Values and Thermodynamic Data of Parallel-Stranded Oligonucleotide Duplexes Containing the Nucleosides* **1**, **2a**–**c**, *and* **3a**–**c**[a])[b])

| | $T_m$ [°C] | $\Delta H^\circ$ [kcal/mol] | $\Delta S^\circ$ [cal/mol K] | $\Delta G^\circ_{310}$ [kcal/mol] |
|---|---|---|---|---|
| 5′-d(TAG GTC AAT ACT)-3′ (**11**)<br>5′-d(ATiC iCAiG TTA TiGA)-3′ (**36**) | 39 | – 74.4 | – 212.3 | – 8.5 |
| 5′-d(T**1**G GTC **11**T **1**CT)-3′ (**31**)<br>5′-d(ATiC iCAiG TTA TiGA)-3′ (**36**) | 36 | – 48.12 | – 129.68 | – 7.90 |
| 5′-d(TAG GTC **2a2a**T ACT)-3′ (**13**)<br>5′-d(ATiC iCAiG TTA TiGA)-3′ (**36**) | 41 | – 61.77 | – 170.95 | – 8.75 |
| 5′-d(TAG GTC **2b2b**T ACT)-3′ (**16**)<br>5′-d(ATiC iCAiG TTA TiGA)-3′ (**36**) | 45 | – 66.59 | – 183.94 | – 9.54 |
| 5′-d(TAG G**3b**C AA**3b** ACT)-3′ (**26**)<br>5′-d(ATiC iCAiG TTA TiGA)-3′ (**36**) | 37 | – 50.64 | – 137.87 | – 7.88 |
| 5′-d(TAG G**3c**C AA**3c** ACT)-3′ (**28**)<br>5′-d(ATiC iCAiG TTA TiGA)-3′ (**36**) | 36 | – 55.09 | – 152.14 | – 7.90 |
| 5′-d(TiCA TAA iCTiG iGAT)-3′ (**37**)<br>5′-d(AGT ATT GAC CTA)-3′ (**12**) | 44 | – 85.0 | – 242.0 | – 10.0 |
| 5′-d(TiCA TAA iCTiG iGAT)-3′ (**37**)<br>5′-d(AGT **1**TT G**1**C CTA)-3′ (**30**) | 39 | – 61.00 | – 169.68 | – 8.38 |
| 5′-d(TiCA TAA iCTiG iGAT)-3′ (**37**)<br>5′-d(AGT **2a**TT G**2a**C CTA)-3′ (**14**) | 45 | – 80 | – 230 | – 10.3 |
| 5′-d(TiCA TAA iCTiG iGAT)-3′ (**37**)<br>5′-d(AGT **2b**TT G**2b**C CTA)-3′ (**17**) | 48 | – 68.34 | – 186.29 | – 10.56 |
| 5′-d(TiCA TAA iCTiG iGAT)-3′ (**37**)<br>5′-d(AGT A**3b3b** GAC CTA)-3′ (**27**) | 43 | – 76.03 | – 215.51 | – 9.19 |
| 5′-d(TiCA TAA iCTiG iGAT)-3′ (**37**)<br>5′-d(ACT A**3c3c** GAC CTA)-3′ (**29**) | 42 | – 67.15 | – 187.02 | – 9.15 |

[a]) Measured at 260 nm in 1M NaCl, 100 mM $MgCl_2$, 60 mM Na-cacodylate buffer, pH 7.0, with 5 μM + 5 μM oligomer concentration. [b]) d(iC) = $m^5iC_d$ = 2′-deoxy-5-methylisocytidine.

induced by the halogenation of the major groove. Apparently, stacking interactions between the nearest neighbors are strengthened in the case of **2b**,**c** but not with **3b**,**c**.

Financial support by the *Deutsche Forschungsgemeinschaft* and the *Roche Diagnostics GmbH* is gratefully acknowledged. We thank Dr. *H. Rosemeyer* and *Y. He* for the NMR measurements, Dr. *T. Wenzel* for the MALDI-TOF spectra, *H. Debelak* for his support in the synthesis of **8a**, *H. Debelak* and *E. Feiling* for the drawings. Compound **10a** was provided by *Y. He*.

## Experimental Part

*General*. See [1][2]. Flash chromatography (FC): 0.4 bar, silica gel *60 H* (*Merck*, Darmstadt, Germany). Thin-layer chromatography (TLC): Aluminium sheets, silica gel *60* $F_{254}$ (0.2 mm, *Merck*, Germany). Solvent systems for FC and TLC: $CH_2Cl_2$/MeOH 9:1 (*A*), $CH_2Cl_2$/MeOH 95:5 (*B*), $CH_2Cl_2$/acetone 9:1 (*C*), $CH_2Cl_2$/AcOEt 85:15 (*D*), $CH_2Cl_2$/acetone 95:5 (*E*). M.p.: *Büchi SMP-20* apparatus (*Büchi*, Switzerland); uncorrected. NMR Spectra: *Avance DPX-250* and *AMX-500* spectrometers (*Bruker*, Germany); $\delta$ values in ppm downfield

from internal $SiMe_4$ ($^1H$, $^{13}C$). Microanalyses were performed by *Mikroanalytisches Labor Beller*, Göttingen, Germany.

*Oligonucleotides.* Oligonucleotide synthesis was performed on a DNA synthesizer, model *392 (Applied Biosystems*, Weiterstadt, Germany). Melting curves were measured with a *Cary 1/3* UV/VIS spectrophotometer (*Varian*, Australia) equipped with a *Cary* thermoelectrical controller. The temp. was measured continuously in the reference cell with a Pt-*100* resistor, and the thermodynamic data of duplex formation were calculated by the Meltwin 3.0 program [30]. CD Spectra: *Jasco 600* (*Jasco*, Japan) spectropolarimeter with thermostatically (*Lauda RCS-6* bath) controlled 1-cm cuvettes. UV Spectra: *150-20* spectrometer (*Hitachi*, Japan); the following extinction coefficients were used ($\varepsilon_{260}$): $^7G_d$ 2700, dT 8800, dC 7300, dA 15400, dG 11700, **2a** 8800, **2b** 8700, **2c** 8700, **3a** 10000, **3b** 4800, **3c** 3700. Snake-venom phosphodiesterase (EC 3.1.15.1, *Crotallus durissus*) and alkaline phosphatase (EC 3.1.3.1, *E. coli*) were generous gifts from *Roche Diagnostics GmbH*, Germany. MALDI-TOF-MS: *Biflex-III* spectrometer (*Bruker Saxonia*, Leipzig, Germany); *Table 10*.

Table 10. *Molecular Masses* ($[M+H]^+$) *of Oligonucleotides Measured by MALDI-TOF Mass Spectrometry*

| | $[M+H]^+$ (calc.) | $[M+H]^+$ (found) |
|---|---|---|
| 5′-d(TAG GTC AAT ACT)-3′ (**11**) | 3644.4 | 3645 |
| 5′-d(AGT ATT GAC CTA)-3′ (**12**) | 3644.4 | 3645 |
| 5′-d(TAG GTC **2a2a**T ACT)-3′ (**13**) | 3674.4 | 3677 |
| 5′-d(AGT **2a**TT G**2a**C CTA)-3′ (**14**) | 3674.4 | 3675 |
| 5′-d(TAG GTC **2b2b**T ACT)-3′ (**16**) | 3832.5 | 3830 |
| 5′-d(AGT **2b**TT G**2b**C CTA)-3′ (**17**) | 3832.5 | 3832 |
| 5′-d(T**2b**G GTC **2b2b**T **2b**CT)-3′ (**18**) | 4020 | 4021 |
| 5′-d(AGT ATT G**2c**C CTA)-3′ (**19**) | 3786 | 3787 |
| 5′-d(AGT **2c**TT GAC CTA)-3′ (**20**) | 3786 | 3792 |
| 5′-d(AGT **2c**TT G**2c**C CTA)-3′ (**21**) | 3926.5 | 3927 |
| 5′-d(TAG GTC **2c2c**T ACT)-3′ (**22**) | 3927 | 3931 |
| 5′-d(T**2c**G GTC **2c2c**T **2c**CT)-3′ (**23**) | 4206.3 | 4210 |
| 5′-d(TAG G**3a**C AA**3a** ACT)-3′ (**24**) | 3613.1 | 3616 |
| 5′-d(AGT A**3a3a** GAC CTA)-3′ (**25**) | 3613.1 | 3615 |
| 5′-d(TAG G**3b**C AA**3b** ACT)-3′ (**26**) | 3774.1 | 3775 |
| 5′-d(AGT A**3b3b** GAC CTA)-3′ (**27**) | 3774.1 | 3772 |
| 5′-d(TAG G**3c**C AA**3c** ACT)-3′ (**28**) | 3868.1 | 3871 |
| 5′-d(AGT A**3c3c** GAC CTA)-3′ (**29**) | 3868.1 | 3871 |

*Synthesis and Purification of Oligonucleotides.* The synthesis was carried out on a 1-μmol scale with the 3′-phosphoramidites of $[(MeO)_2Tr]ib^2G_d$, $[(MeO)_2Tr]bz^6A_d$, $[(MeO)_2Tr]bz^4C_d$, and $[(MeO)_2Tr]T_d$ for the synthesis of oligonucleotides containing **2a**–**c**, and $[(MeO)_2Tr]tac^2G_d$, $[(MeO)_2Tr]tac^6A_d$, $[(MeO)_2Tr]tac^4C_d$, and $[(MeO)_2Tr]T_d$ for the synthesis of oligonucleotides containing **3a**–**c**. After cleavage of the oligonucleotides from the solid support, the former were deprotected in 25% aq. $NH_3$ soln. for 12–15 h at 60°. The latter were incubated in 25% aq. $NH_3$ soln. for 1.5–2 h at r.t. for deprotection. Purification of the 5′-(dimethoxytrityl)-oligomers was performed by reversed-phase HPLC (*RP-18*). The following solvent gradient was used (*A*, 0.1M $(Et_3NH)OAc$ (pH 7.0)/MeCN 95:5; *B*, MeCN): 3 min 20% *B* in *A*, 12 min 20–40% *B* in *A* with a flow rate of 1.0 ml/min. The concentrated oligonucleotide solns. were treated with 2.5% $CHCl_2COOH/CH_2Cl_2$ for 5 min at r.t. to remove the 4,4′-dimethoxytrityl residues. The detritylated oligomers were purified by reversed-phase HPLC with the gradient: 20 min 0–20% *B* in *A* with a flow rate of 1 ml/min. The oligomers were desalted on a short column (*RP-18*, silica gel) and then lyophilized on a *Speed-Vac* evaporator to yield colorless solids, which were frozen at −24°.

*Nucleoside-Composition Analysis.* The oligonucleotides were dissolved in 0.1M *Tris*·HCl buffer (pH 8.3, 200 μl), and treated with snake-venom phosphodiesterase (3 μl) at 37° for 45 min, and then alkaline phosphatase (3 μl) at 37° for another 30 min. The mixtures were analyzed on reversed-phase HPLC (*RP-18*, at 260 nm, gradient *A*, 0.7 ml/min). The retention time of **2a**–**c** and **3a**–**c** were used as standards (*Fig. 1*). The extinction coefficients of the nucleosides and the peak areas were used for quantification of the composition of the oligonucleotides (*Fig. 1, a–d*).

*1-(2-Deoxy-β-*D*-*erythro*-pentofuranosyl)-3-iodo-1*H*-pyrazolo[3,4-*d*]pyrimidine-4,6-diamine* (**2c**). A soln. of 1-(2-deoxy-β-D-*erythro*-pentofuranosyl)-3-iodo-4-isopropoxy-1*H*-pyrazolo[3,4-*d*]pyrimidin-6-amine (**4**) [11] (1 g, 2.3 mmol) in aq. 25% $NH_3$ soln. (80 ml) was heated at 70° in an autoclave for 4 d. The solvent was evaporated and the residue dissolved in hot $H_2O$ and crystallized. Colorless needles (640 mg, 71%). M.p. 154°. TLC (*A*): $R_f$ 0.2. UV (MeOH): 223 (31800), 260 (8700), 278 (9100). $^1$H-NMR ($(D_6)$DMSO): 2.12 (*m*, $H_\alpha$–C(2′)); 2.67 (*m*, $H_\beta$–C(2′)); 3.38, 3.44 (*m*, 2 H–C(5′)); 3.73 (*m*, H–C(4′)); 4.33 (*m*, H–C(3′)); 4.73 (*t*, *J* = 5.7, OH–C(5′)); 5.17 (*d*, *J* = 4.3, OH–C(3′)); 6.27 (‘*t*’, *J* = 6.5, H–C(1′)); 6.34 (br., $NH_2$); 6.62 (br., $NH_2$). Anal. calc. for $C_{10}H_{13}IN_6O_3$ (392.2): C 30.63, H 3.34, N 21.43; found: C 30.91, H 3.61, N 21.27.

*3-Bromo-1-(2-deoxy-β-*D*-*erythro*-pentofuranosyl)-N$^4$,N$^6$-bis(2-methylpropanoyl)-1*H*-pyrazolo[3,4-*d*]pyrimidine-4,6-diamine* (**5a**). Compound **2b** [5] (0.74 g, 2.14 mmol) was co-evaporated with anh. pyridine (3×) and then dissolved in anh. pyridine (5 ml), while stirring at r.t. $Me_3SiCl$ (1.37 ml, 10.8 mmol), and after 15 min, isobutyric anhydride (3.56 ml, 21.5 mmol) were added. Stirring was continued for 3 h. The mixture was cooled in an ice-bath and diluted with $H_2O$ (2.5 ml); 5 min later, aq. 25% $NH_3$ soln. (4.3 ml) was added. After stirring for 30 min, the mixture was evaporated and co-evaporated with toluene (3×). The residue was purified by FC ($CH_2Cl_2$/MeOH 9 :1), furnishing two zones. From the fast migrating zone, **5a** was obtained as a colorless amorphous solid (500 mg, 48%). $R_f$ (*A*) 0.4. UV (MeOH): 284 (9500), 239 (33900). $^1$H-NMR ($(D_6)$DMSO): 1.15 (*m*, 2 *Me*$_2$CH); 2.25 (*m*, $H_\alpha$–C(2′)); 2.75 (*m*, $H_\beta$–C(2′)); 2.86 (*m*, 2 Me$_2$C*H*); 3.47 (*m*, 2 H–C(5′)); 3.81 (*m*, H–C(4′)); 4.44 (*m*, H–C(3′)); 4.73 (*t*, *J* = 5.5, OH–C(5′)); 5.32 (*d*, *J* = 4.3, OH–C(3′)); 6.54 (‘*t*’, *J* = 6.6, H–C(1′)); 10.59, 10.72 (2*s*, 2 NH). Anal. calc. for $C_{18}H_{25}BrN_6O_5$ (485.3): C 44.55, H 5.19, N 17.32; found: C 44.90, H 5.28, N 16.81.

*3-Bromo-1-(2-deoxy-β-*D*-*erythro*-pentofuranosyl)-N$^6$-(2-methylpropanoyl)-1*H*-pyrazolo[3,4-*d*]pyrimidine-4,6-diamine* (**6**). The slower migrating zone from the above reaction afforded **6** as a colorless amorphous solid (0.2 g, 22%). $R_f$ (*A*) 0.36. UV (MeOH): 283 (10900), 237 (49500). $^1$H-NMR ($(D_6)$DMSO): 1.04, 1.07 (*m*, *Me*$_2$CH); 2.21 (*m*, $H_\alpha$–C(2′)); 2.71 (*m*, $H_\beta$–C(2′)); 2.90 (*m*, Me$_2$C*H*); 3.46 (*m*, 2 H–C(5′)); 3.78 (*m*, H–C(4′)); 4.38 (*m*, H–C(3′)); 4.72 (*t*, *J* = 5.6, OH–C(5′)); 5.28 (*d*, *J* = 4.3, OH–C(3′)); 6.42 (‘*t*’, *J* = 6.4, H–C(1′)); 6.96, 7.76 (br., $NH_2$); 10.08 (br., NH). Anal. calc. for $C_{14}H_{19}BrN_6O_4$ (415.2): C 40.49, H 4.61, N 20.24; found: C 40.58, H 4.72, N 19.93.

N$^4$,N$^6$-*Dibenzoyl-1-(2-deoxy-β-*D*-*erythro*-pentofuranosyl)-3-iodo-1*H*-pyrazolo[3,4-*d*]pyrimidine-4,6-diamine* (**5b**). Compound **2c** (1.0 g, 2.55 mmol) was co-evaporated twice with toluene. The residue was dissolved in anh. pyridine (40 ml), and $Me_3SiCl$ (3.25 ml, 25.5 mmol) was added while stirring. The mixture was stirred under Ar, cooled to 0°, and PhCOCl (3.0 ml, 25.8 mmol) was added dropwise within 30 min. After stirring overnight at r.t., the mixture was diluted with AcOEt (200 ml), the org. phase washed with sat. aq. $NaHCO_3$ soln. (200 ml) and ice-cold $H_2O$ (200 ml), the aq. phase extracted with AcOEt (2 × 400 ml), the combined org. phase evaporated, and the residue dissolved in THF/MeOH/$H_2O$ 5 :4 :1 (250 ml). The dark orange soln. was cooled to 0°, then 2N NaOH (25 ml) was added, and stirring was continued for another 40 min. The residue was purified by FC ($CH_2Cl_2$/MeOH 98 :2 → $CH_2Cl_2$/MeOH 95 :5): **5b** (1.15 g, 75%). Amorphous solid. TLC (*B*): $R_f$ 0.4. UV (MeOH): 244 (17400), 276 (14200). $^1$H-NMR ($(D_6)$DMSO): 2.13 (*m*, $H_\alpha$–C(2′)); 2.67 (*m*, $H_\beta$–C(2′)); 3.38, 3.52 (*m*, 2 H–C(5′)); 3.84 (*m*, H–C(4′)); 4.46 (*m*, H–C(3′)); 4.72 (*t*, *J* = 5.7, OH–C(5′)); 5.29 (*d*, *J* = 4.4, OH–C(3′)); 6.66 (‘*t*’, *J* = 6.5, H–C(1′)); 7.51–8.11 (*m*, arom. H); 10.54, 10.78 (*s*, 2 NH). Anal. calc. for $C_{24}H_{21}IN_6O_5$ (586.4): C 48.01, H 3.53, N 14.00; found: C 47.93, H 3.53, N 14.05.

*3-Bromo-1-[2-deoxy-5-*O*-(4,4′-dimethoxytrityl)-β-*D*-*erythro*-pentofuranosyl]-N$^4$,N$^6$-bis(2-methylpropanoyl)-1*H*-pyrazolo[3,4-*d*]pyrimidine-4,6-diamine* (**7a**). Compound **5a** (0.5 g, 1.03 mmol) was co-evaporated with anh. pyridine (3×) and dissolved in pyridine (1.5 ml). $(MeO)_2TrCl$ (0.45 g, 1.33 mmol) was added, and the mixture was stirred at r.t. for 3 h. The reaction was quenched by addition of MeOH, and the mixture evaporated and co-evaporated with toluene (3×). FC ($CH_2Cl_2$/MeOH 10 :1) gave **7a**. Colorless foam (0.57 g, 70%). $R_f$ (*B*) 0.3. UV (MeOH): 237 (52000), 283 (10500). $^1$H-NMR ($(D_6)$DMSO): 1.04–1.17 (*m*, 2 *Me*$_2$CH)); 2.29 (*m*, $H_\alpha$–C(2′)); 2.85 (*m*, $H_\beta$–C(2′)); 2.89 (*m*, 2 Me$_2$C*H*)); 3.07 (*m*, 2 H–C(5′)); 3.71 (*s*, 2 MeO); 3.94 (*m*, H–C(4′)); 4.46 (*m*, H–C(3′)); 5.35 (*m*, OH–C(3′)); 6.57 (*m*, H–C(1′)); 10.57, 10.74 (*s*, 2 NH). Anal. calc. for $C_{39}H_{43}BrN_6O_7$ (787.2): C 59.47, H 5.46, N 10.67; found: C 59.08, H 5.37, N 10.39.

*3-Bromo-1-[2-deoxy-5-*O*-(4,4′-dimethoxytrityl)-β-*D*-*erythro*-pentofuranosyl]-N$^4$,N$^6$-bis(2-methylpropanoyl)-1*H*-pyrazolo[3,4-*d*]pyrimidine-4,6-diamine 3′-(2-Cyanoethyl Diisopropylphosphoramidite)* (**8a**). To a soln. of **7a** (0.24 g, 0.3 mmol) in anh. $CH_2Cl_2$ (3 ml) under Ar, $^i$Pr$_2$EtN (0.16 ml, 0.9 mmol) and 2-cyanoethyl diisopropylphosphoramidochloridite (91 µl, 0.41 mmol) were added, and the mixture was stirred at r.t. for 30 min (TLC monitoring). Then, the mixture was diluted with $CH_2Cl_2$ and the soln. washed with 5% aq. $NaHCO_3$ soln. (2×) and brine. The org. phase was dried ($Na_2SO_4$) and evaporated and the product separated by FC: **8a** (193 mg, 65%). Colorless foam. $R_f$ (*E*) 0.63, 0.69. UV (MeOH): 282 (10000), 237 (49500). $^1$H-NMR

((D$_6$)DMSO): 1.11–1.35 (*m*, 4 *Me*$_2$CH); 2.51 (*m*, H$_\alpha$–C(2′)); 2.66 (*m*, H$_\beta$–C(2′)); 2.95–3.91 (*m*, 2 H–C(5′), 2 Me$_2$C*H*, CH$_2$CH$_2$); 3.80 (*s*, MeO); 4.26 (*m*, H–C(4′)); 4.82 (*m*, H–C(3′)); 6.71 (*m*, H–C(1′)); 6.75–7.44 (*m*, arom. H); 8.39, 8.59 (br., 2 NH). $^{31}$P-NMR (CDCl$_3$), 149.61, 149.65. Anal. calc. for $C_{48}H_{60}BrN_8O_8P$ (921.2): C 58.36, H 6.08, N 11.35; found: C 58.86, H 6.18, N 11.55.

N$^4$,N$^6$-*Dibenzoyl-1-[2-deoxy-5*-O-*(4,4′-dimethoxytrityl)-β*-D-erythro-*pentofuranosyl]-3-iodo-1*H-*pyrazolo[3,4*-d*]pyrimidine-4,6-diamine* (**7b**). Compound **5b** (450 mg, 0.75 mmol) was co-evaporated twice with anh. pyridine. The residue was dissolved in pyridine (2 ml), and dimethoxytrityl chloride (305 mg, 0.9 mmol) was added. After 4 h stirring, the soln. was diluted with 5 ml of MeOH and washed with 5% aq. NaHCO$_3$ soln. (3 × 20 ml). The org. phase was dried (Na$_2$SO$_4$) and evaporated. The residue was purified by FC (CH$_2$Cl$_2$/acetone 95:5 → CH$_2$Cl$_2$/acetone 9:1): 375 mg (55%) of **7b**. Colorless foam. $R_f$ (*C*) 0.4. UV (MeOH): 244 (16900), 276 (16200). $^1$H-NMR ((D$_6$)DMSO): 2.35 (*m*, H$_\alpha$–C(2′)); 2.67 (*m*, H$_\beta$–C(2′)); 3.07, 3.09 (2*m*, 2 H–C(5′)); 3.70 (*s*, 2 MeO); 3.96 (*m*, H–C(4′)); 4.56 (*m*, H–C(3′)); (*d*, *J* = 4.8, OH–C(3′)); 6.72–8.11 (*m*, arom. H); 10.54, 10.78 (2*s*, 2 NH). Anal. calc. for $C_{45}H_{39}IN_6O_7$ (902.73): C 59.87, H 4.35, N 9.31; found: C 59.93, H 4.33, N 9.39.

N$^4$,N$^6$-*Dibenzoyl-1-[2-deoxy-5*-O-*(4,4′-dimethoxytrityl)-β*-D-erythro-*pentofuranosyl]-3-iodo-1*H-*pyrazolo[3,4*-d*]pyrimidine-4,6-diamine 3′-(2-Cyanoethyl Diisopropylphosphoramidite)* (**8b**). Compound **7b** (330 mg, 0.37 mmol) was dissolved in THF (5 ml). $^i$Pr$_2$EtN (186 µl, 1.07 mmol) and 2-cyanoethyl diisopropylphosphoramidochloridite (108 µl, 0.48 mmol) were added under Ar. After 30 min, the mixture was diluted with CH$_2$Cl$_2$ (20 ml) and 5% aq. NaHCO$_3$ soln. (2 × 20 ml). The mixture was extracted with CH$_2$Cl$_2$ (3 × 15 ml), the combined org. layer dried (Na$_2$SO$_4$) and evaporated, and the oily residue submitted to FC (CH$_2$Cl$_2$/AcOEt 85:15): 280 mg (69%) of **8b**. Colorless foam. $R_f$ (*D*) 0.8. $^{31}$P-NMR (CDCl$_3$): 149.37, 149.38.

## REFERENCES


[1] F. Seela, G. Becher, *Helv. Chim. Acta* **2000**, *83*, 928; F. Seela, G. Becher, M. Zulauf, *Nucleosides Nucleotides* **1999**, *18*, 1399.
[2] F. Seela, M. Zulauf, *J. Chem. Soc., Perkin Trans. 1* **1999**, 479.
[3] F. Seela, G. Becher, *Helv. Chim. Acta* **1999**, *82*, 1640.
[4] N. Ramzaeva, F. Seela, *Helv. Chim. Acta* **1996**, *79*, 1549.
[5] F. Seela, G. Becher, *Nucleic Acids Res.* **200**, *29*, in press.
[6] C. Cheong, I. J. Tinoco, A. Chollet, *Nucleic Acids Res.* **1988**, *16*, 5115.
[7] C. Bailly, M. J. Waring, *Nucleic Acids Res.* **1998**, *26*, 4309 and ref. cit. therein.
[8] J. Sági, E. Szakonyi, M. Vorlickova, J. Kypr, *J. Biomolec. Struct. Dyn.* **1996**, *13*, 1035.
[9] F. Seela, M. Zulauf, *Chem.–Eur. J.* **1998**, *4*, 1781.
[10] A. Bondi, *J. Phys. Chem.* **1964**, *68*, 441.
[11] F. Seela, G. Becher, *Synthesis* **1998**, *2*, 207.
[12] J. Asakua, M. J. Robins, *J. Org. Chem.* **1990**, *55*, 4928.
[13] J. van Wijk, C. Altona, 'PSEUROT 6.2 – A Program for the Conformational Analysis of the Five-Membered Rings', University of Leiden, July, 1993.
[14] F. Seela, G. Becher, H. Rosemeyer, H. Reuter, G. Kastner, I. A. Mikhailopulo, *Helv. Chim. Acta* **1999**, *82*, 105.
[15] G. Blackburn, M. J. Gait, 'Nucleic Acids in Chemistry and Biology', IRL Press, Oxford University Press, 1990, p. 28.
[16] C. Thibaudeau, J. Plavec, J. Chattopadhyaya, *J. Org. Chem.* **1996**, *61*, 266.
[17] G. S. Ti, B. L. Gaffney, R. A. Jones, *J. Am. Chem. Soc.* **1982**, *104*, 1316.
[18] I. Luyten, A. V. Aerschot, J. Rozenski, R. Busson, P. Herdewijn, *Nucleosides Nucleotides* **1997**, *16*, 1649.
[19] Y. S. Sanghvi, G. D. Hoke, S. M. Freier, M. C. Zounes, C. Gonzalez, L. Cummins, H. Sasmor, P. D. Cook, *Nucleic Acids Res.* **1993**, *21*, 3197.
[20] S. L. Beaucage, M. Caruthers, *Tetrahedron Lett.* **1981**, *22*, 1859.
[21] E. Ferrer, C. Fàbrega, R. G. Garcia, F. Azorín, R. Eritja, *Nucleosides Nucleotides* **1996**, *15*, 907; J. C. Schulhof, D. Molko, R. Teoule, *Nucleic Acids Res.* **1987**, *15*, 397; R. D. Sheardy, N. C. Seeman, *J. Org. Chem.* **1986**, *51*, 4301.
[22] Applied Biosystems, 'User's Manual for Oligonucleotide Purification Cartridges'.
[23] F. Seela, C. Wei, *Helv. Chim. Acta* **1999**, *82*, 726.
[24] J. D. Hoheisel, H. Lehrach, *FEBS Lett.* **1990**, *274*, 103.

[25] S. M. Freier, K.-H. Altman, *Nucleic Acids Res.* **1997**, *25*, 4429.
[26] F. Seela, Y. He, *Helv. Chim. Acta* **2000**, *83*, 2527; S. Wang, E. T. Kool, *Biochemistry* **1995**, *34*, 4125.
[27] B. C. Froehler, S. Wadwani, T. J. Terhorst, S. R. Gerrard, *Tetrahedron* **1992**, *33*, 5307.
[28] N. Ramzaeva, C. Mittelbach, F. Seela, *Helv. Chim. Acta* **1997**, *80*, 1809.
[29] F. Seela, C. Wei, G. Becher, M. Zulauf, P. Leonard, *Bioorg. Med. Chem. Lett*. **2000**, *10*, 289.
[30] J. A. McDowell, D. H. Turner, *Biochemistry* **1996**, *35*, 14077.

*Received February 13, 2001*